The Astrophysical Journal, 825:121 (8pp), 2016 July 10 doi:10.3847/0004-637X/825/2/121

POWER SPECTRAL DENSITY OF FLUCTUATIONS OF BULK AND THERMAL SPEEDS IN THE SOLAR WIND

J. Šafránková[1], Z. Němeček[1], F. Němec[1], L. Přech[1], C. H. K. Chen[2], and G. N. Zastenker[3]
[1] Charles University, Faculty of Mathematics and Physics, V Holešovičkách 2, 180 00 Prague 8, Czech Republic; jana.safrankova@mff.cuni.cz
[2] Department of Physics, Imperial College London, London SW7 2AZ, UK
[3] Space Research Institute of Russian Academy of Sciences, Moscow, Russia, Profsoyuznaya ul. 84/32, Moscow 117997, Russia
Received 2016 March 23; revised 2016 May 2; accepted 2016 May 2; published 2016 July 11

ABSTRACT

This paper analyzes solar wind power spectra of bulk and thermal speed fluctuations that are computed with a time resolution of 32 ms in the frequency range of 0.001–2 Hz. The analysis uses measurements of the Bright Monitor of the Solar Wind on board the *Spektr-R* spacecraft that are limited to 570 km s^{-1} bulk speed. The statistics, based on more than 42,000 individual spectra, show that: (1) the spectra of bulk and thermal speeds can be fitted by two power-law segments; (2) despite their large variations, the parameters characterizing frequency spectrum fits computed on each particular time interval are very similar for both quantities; (3) the median slopes of the bulk and thermal speeds of the segment attributed to the MHD scale are −1.43 and −1.38, respectively, whereas they are −3.08 and −2.43 in the kinetic range; (4) the kinetic range slopes of bulk and thermal speed spectra become equal when either the ion density or magnetic field strength are high; (5) the break between MHD and kinetic scales seems to be controlled by the ion β parameter; (6) the best scaling parameter for bulk and thermal speed variations is a sum of the inertial length and proton thermal gyroradius; and (7) the above conclusions can be applied to the density variations if the background magnetic field is very low.

Key words: solar wind – turbulence

1. INTRODUCTION

The solar wind plasma is a strongly turbulent environment with electromagnetic fields and plasma properties that fluctuate over a wide range of timescales. To understand the physical mechanisms of solar wind turbulence, various topics have been addressed: the nature and properties of the fluctuations, the origin and evolution of turbulence in the interplanetary medium, the mechanisms of the turbulent cascade of energy, dissipation at the smallest scales, etc.

Observations of the solar wind magnetic field have shown that the magnetic power spectral density is a power law of approximately $k^{-5/3}$ at large scales in the inertial range (e.g., Matthaeus & Goldstein 1982; Bruno & Carbone 2013), where aspects of the MHD approximation can be used (Biskamp 1993), as predicted by Goldreich & Sridhar (1995). At frequencies corresponding to the scale of the proton Larmor radius, the turbulent fluctuations become more compressible (Leamon et al. 1998; Alexandrova et al. 2008; Chen et al. 2012; Salem et al. 2012; Kiyani et al. 2013), the spectra exhibit a break, and the density fluctuation spectrum exhibits a local flattening. Magnetic spectra are variable and ion instabilities occur as a function of the local plasma parameters.

Between ion and electron scales, a small-scale turbulent cascade of the magnetic energy from proton scales, where kinetic properties of ions do not meet fluid approximations, is characterized by a steeper power law with a spectral index varying between −2 and −4 (e.g., Leamon et al. 1998; Smith et al. 2006; Alexandrova et al. 2008, 2009; Sahraoui et al. 2009). Recently, a power-law spectrum of magnetic and density fluctuations with a spectral index close to −2.8 seems to have been established (e.g., Chen et al. 2012; Bruno & Carbone 2013; Howes 2015; Riazantseva et al. 2015; Šafránková et al. 2015).

On the other hand, measurements have shown that the spectral indices of the magnetic field and velocity fluctuations are different in the inertial scale. The magnetic field exhibits an average spectral index close to −5/3 (e.g., Podesta & Borovsky 2010; Boldyrev et al. 2011a; Chen et al. 2011; Borovsky 2012); however, Grappin et al. (1991) reported that the velocity spectra are systematically less steep than the magnetic field spectra. Later, the spectral slope of velocity fluctuations very close to −3/2 was confirmed as presented by many authors who used different spacecraft data and various techniques of spectral analysis (Mangeney et al. 2001; Salem et al. 2007; Podesta et al. 2006, 2007; Podesta & Borovsky 2010; Boldyrev et al. 2011b; Chen et al. 2011, 2013a).

An analysis of the spectra at different distances from the Sun shows that the velocity field evolves more rapidly than the magnetic field (Roberts 2010) due to the dominance of the magnetic energy over the kinetic at inertial range scales (e.g., Belcher & Davis 1971; Podesta et al. 2007; Salem et al. 2009; Chen et al. 2011; Wang et al. 2011). The difference between magnetic and kinetic energies is usually called residual energy. Currently, it is thought that the residual energy in the solar wind fluctuations can be injected by driving or can arise from turbulent interactions (Chen et al. 2013a). The residual energy has been shown to follow the scaling of the total energy spectrum (Grappin et al. 1983; Muller & Grappin 2005; Boldyrev & Perez 2009, 2012; Chen et al. 2013a); however, the residual energy spectrum (in the kinetic normalization) was found to be steeper than the total energy as well as the velocity and magnetic field spectra. Its spectral index was found to be close to −1.9 (Boldyrev et al. 2011a), consistent with MHD turbulence predictions and numerical simulations. Boldyrev & Perez (2009) proposed that weak turbulence naturally generates a condensate of residual energy in small parallel wavenumber modes.

Šafránková et al. (2013a) have shown that the fluctuations of the bulk and thermal speeds are similar to each other and that the spectral indices differ from those determined for the density

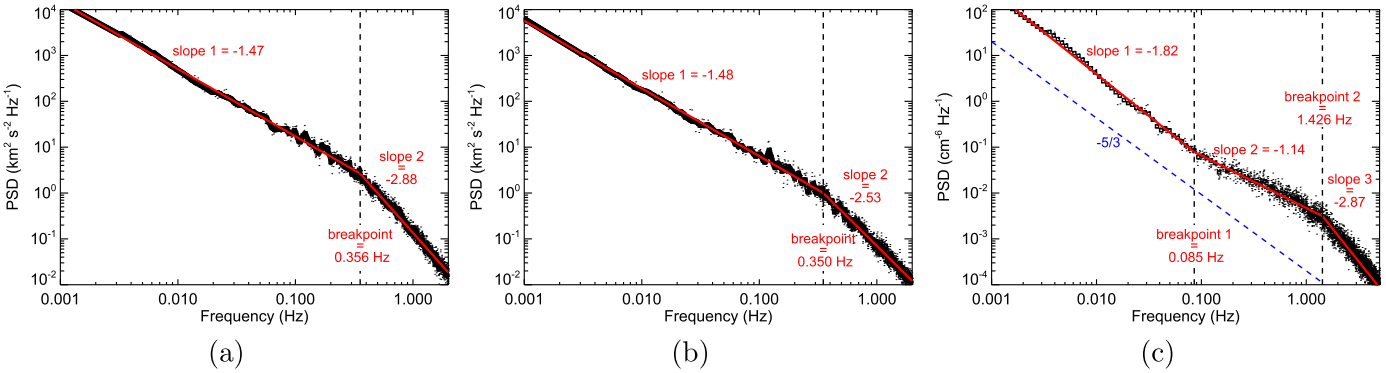

Figure 1. Example of the solar wind spectra on 2012 July 6 between 1600 and 1900 UT: (a) the frequency spectra of the proton bulk speed; (b) proton thermal speed; and (c) ion density. In the panels, the original spectra are shown as small black dots; the rectangles stand for smoothed values; the fits of the spectra are highlighted by the red broken line; and values of the spectral slopes and breaks are given in each panel.

fluctuations (Chen et al. 2014b; Šafránková et al. 2015). At the MHD scale, the slope of −1.45 for the speed spectrum was consistent with the finding of other authors (Podesta et al. 2006, 2007; Podesta & Borovsky 2010; Boldyrev et al. 2011b; Chen et al. 2011). From the first measurements of the bulk and thermal speed fluctuations at the ion kinetic scale, Šafránková et al. (2013a) found that both speeds exhibit a steeper spectrum with mean slopes of about −3.4 and that the deviation between the density and speed spectral indices results in different ion break frequencies.

In situ solar wind measurements near ion scales have been rare up to now, and thus the purpose of this investigation is to estimate the power-law exponents and ion break frequency of the bulk and thermal velocity fluctuations at kinetic scales. We discuss their spectral properties and dependencies on solar wind parameters and compare them with density fluctuations. This systematic study is based on a relatively large set of the plasma data from the Bright Monitor of Solar Wind (BMSW) instrument that was launched on board the *Spektr-R* spacecraft. The solar wind measurements originate from 2011 August to 2014 December; however, the measurements exhibit some limitations: (1) observations are not continuous, (2) the instrument can register the solar wind velocity up to ≈570 km s^{-1}, and (3) the on board magnetometer is not in operation.

The spectral behavior of magnetic field or velocity fluctuations is usually analyzed using the sum of the power spectral densities of all three components. This approach reflects the properties of compressive as well as Alfvénic fluctuations. Since we would like to compare the results of this study of velocity fluctuations with a similar analysis of density fluctuations (Šafránková et al. 2015) that are compressive, we apply the velocity magnitude as a comparable quantity.

2. DATA PREPARATION AND PROCESSING

The BMSW instrument provides values of the solar wind ion density, proton bulk velocity vector, and thermal speed with a time resolution of ≈32 ms. To achieve this time resolution, only six points of the integral distribution function are measured by six Faraday cups and the solar wind parameters are computed assuming a drifting Maxwellian distribution. The instrument principles and the methods of determining the distribution function moments can be found in Šafránková et al. (2013b). Although the time resolution is sufficient for the determination of spectral properties up to 16 Hz, Šafránková et al. (2015) limited the statistical analysis of ion density frequency spectra to 8 Hz in order to avoid an influence of the instrumental noise on the shape of the spectra. However, computations of the speed and temperature are based on the derivative of the Faraday cup deceleration characteristics and this process increases the noise in the processed data. For this reason, the present study is limited to 2 Hz only. The study is focused on the spectral properties around the break between MHD and ion kinetic scales and Šafránková et al. (2013a) have shown that this break can be expected between 1.5 and 0.3 Hz under typical solar wind conditions. This means that a 2 Hz limit is sufficient for a reliable determination of the break frequency as well as for an estimation of the spectral slopes in both ranges.

The low-frequency limit (0.001 Hz) is determined by the length of the analyzed intervals, which was set to 20 minutes. This duration was chosen as a compromise between the noise in the frequency spectrum that increases with decreasing interval length and variations of the background parameters. These variations can influence turbulence at shorter scales, which is the main subject of the present study.

FFT spectra computed on short time intervals (20 minutes are equal to about 4×10^4 data points) are often noisy and different techniques can be used to smooth them. We follow the approach of Šafránková et al. (2015) using a two-step procedure: (1) A set of overlapped 20 minute basic subintervals is created and the FFT is computed at each subinterval. The overlapping duration is 19 minutes and thus, for example, a 1 hr interval of continuous measurements provides 40 basic subintervals. (2) The whole frequency interval (0.001–2 Hz) is divided into 1000 equidistant parts on a logarithmic scale. Since we expect a power-law spectrum, we do not use the mean values or medians but we fit all points falling into a given frequency interval with a straight line and apply the value of the fit in the middle of a particular interval as a smoothed value. The automated routine fits each individual smoothed spectrum with two power-law functions and the break point is determined as the frequency corresponding to their intersection. The values of power indices and frequencies of break points, together with the averaged values of basic parameters like the magnetic field magnitude, ion density, speed, and temperature, and their standard deviations, create a database for further statistical processing. As noted, magnetic field measurements are not available on board *Spektr-R*, and thus we use the propagated *Wind* magnetic field observations as a proxy.

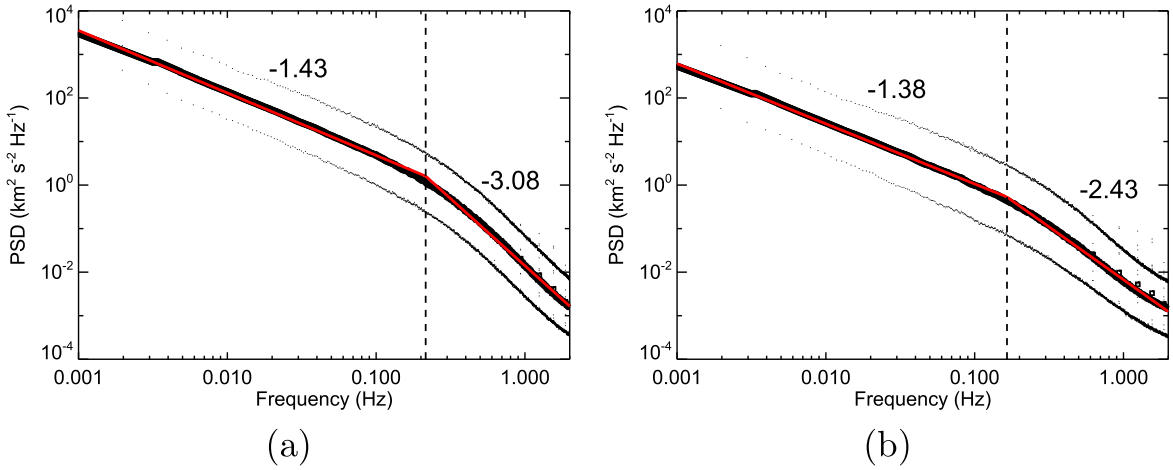

Figure 2. Median power spectral density of the bulk (a) and thermal (b) speeds as a function of the spacecraft frame frequency. The red lines display linear fits, and the values of their slopes are given within the panels. The first and third quartiles are given as scatter estimates.

This way of smoothing is very effective, as can be seen in Figure 1 (see Šafránková et al. 2015 for a discussion of different methods of smoothing). The figure compares frequency spectra of the proton bulk speed (panel 1(a)), proton thermal speed (panel 1(b)), and ion density (panel 1(c)) computed on the time interval of 1600–1900 UT, 2012 July 6. Note that 160 individual spectra overlap in the figure and the corresponding PSDs are shown by the small black dots. The smoothed values are shown by the black rectangles. Since the smoothing described above uses 1000 values, the rectangles merge in one black thick line and the individual points can be distinguished only at the frequencies above 1 Hz or in the density panel (panel (c)). This panel is given for comparison and uses only 100 subintervals for smoothing. The smoothed spectra of speeds are then fitted with two (the density spectrum in the panel 1(c) with three) straight lines and these fits are shown with red lines. Corresponding slopes and breaks are given in particular panels.

The density spectrum exhibits all features described by Chen et al. (2013b) and Šafránková et al. (2015), namely, it consists of three power-law segments that are divided by two break points. By contrast, only two linear parts and one break point can be identified in the frequency spectra of bulk and thermal speeds in Figures 1(a) and (b). The overall shapes of these two spectra are very similar and the differences between the parameters of the fits are within the fit errors with the exception of Slope 2, which is steeper for the bulk than for the thermal speed. The frequency of the break point of the bulk (thermal) speed spectrum is at a lower frequency than break point 2 of the density spectrum, consistent with the preliminary study of Šafránková et al. (2013a).

3. MEDIAN FREQUENCY SPECTRA

Figure 2 presents medians of all frequency spectra of bulk and thermal speeds in our data set. The figure is analogous to Figure 1 but Figure 1 uses one time interval that was carefully chosen as the pristine solar wind without large disturbances and located sufficiently far away from the bow shock. By contrast, all available solar wind measurements are shown in Figure 2. This means that a part of the spectra belongs to intervals in the weak foreshock, downstream of IP shocks or within ICMEs. The only criterion for the selection of intervals was that the spacecraft was upstream of the bow shock. All selected time series were then broken into 20 minute subintervals, FFTs were computed, and the spectra were fitted with two power-law functions. The plausibility of the fits was quantified using a χ square; note that about 15% of the spectra were eliminated from the set. We have checked these spectra and found that they correspond to foreshock intervals or intervals containing IP shocks and similar strong discontinuities.

The fits shown by the red lines reveal that the similarity of the bulk and thermal speeds shown in Figure 1 is a typical feature. The slopes in the MHD range are around -1.4, i.e., close to the value of -1.5 suggested by Podesta et al. (2006, 2007) for the bulk velocity. The break between the MHD and kinetic ranges is at about 0.2 Hz for both quantities but Slope 2, corresponding to the ion kinetic range, is different, being near -3.1 for the bulk and only about -2.4 for the thermal speed, respectively.

A good correspondence of the bulk and thermal speed spectra is shown in Figure 3. The panels of this figure show the parameters describing the shape of the thermal speed spectra (break point, Slope 1, and Slope 2) as a function of the same parameter of the bulk speed spectrum. Each particular spectrum is shown by a small black dot, the red heavy lines stand for the medians computed in the range of a particular parameter and the second and third quartiles are denoted by the red dashed lines. The Spearman rank correlation coefficient is given above the particular panel. This coefficient is equal to 1 if the two variables are monotonically related. Since we are analyzing approximately 42,000 individual spectra, the significance level of all values of the correlation coefficient are above 99%. Note that this comment is valid to all correlations given in the present paper.

The spectra were computed on short intervals and they are rather noisy, which results in a spread of their parameters. Nevertheless, the correlation coefficients exceed 0.7 in all panels. The largest correlation coefficient is for the break point between scales (Figure 3(a)) and we can conclude that these breaks are controlled by the same mechanism. The same is true for Slope 1, which corresponds to the range of MHD fluctuations. This slope is around -1.5 (between -1 and -2) in a great majority of the cases but even rare events with slopes in the range from -1 to 0 exhibit the same trend (Figure 3(b)).

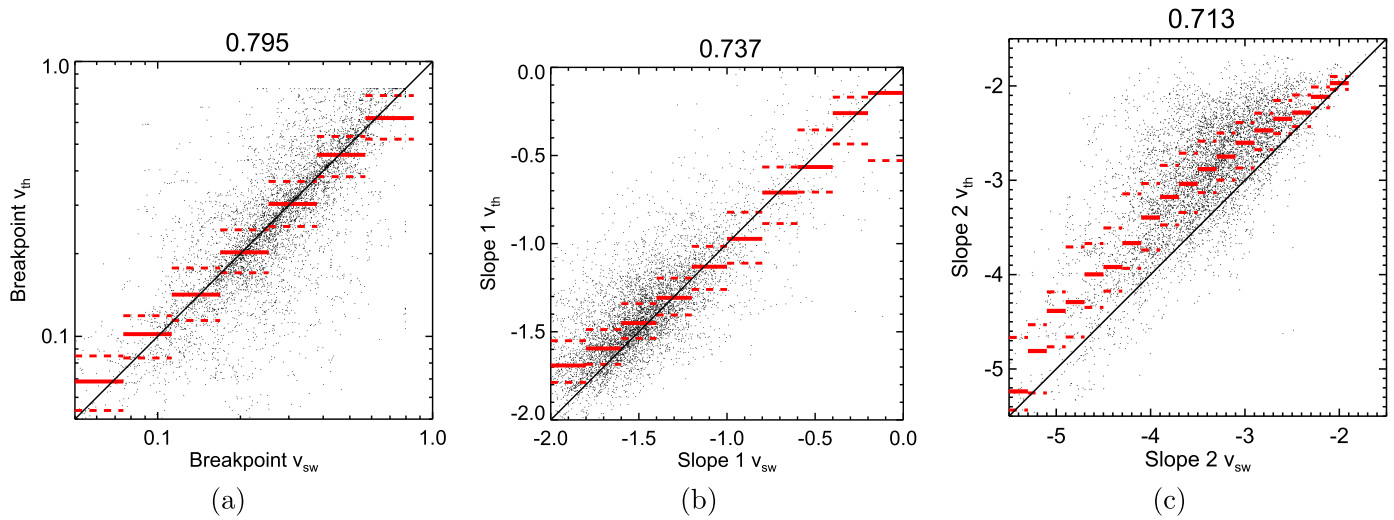

Figure 3. Slopes 1 and 2 and break points of the bulk speed spectra, respectively, as a function of the same quantity of the thermal speed spectra. The segments of the red thick line show medians in particular bins and dashed segments stand for first and third quartiles. The Spearman rank correlation coefficients are given in the top part of each panel. The diagonal black lines indicate an equality of the given quantities.

The only systematic difference between bulk and thermal speed velocity spectra is shown in Figure 3(c). This panel compares the slopes corresponding to the kinetic range and one can see that the steeper slope of the bulk speed spectrum shown in Figure 2 is a typical feature found for the majority of the analyzed intervals. The difference between power indices of bulk and thermal speeds is about 0.5 and it holds nearly in the whole range of observed slopes. The difference apparently decreases for the slopes around -2.5 but the number of such gradual spectra is rather small. Nevertheless, we will return to this point in the discussion.

4. SCALING OF FLUCTUATIONS

The previous section demonstrated a very similar behavior of thermal and bulk speed fluctuations; thus we will analyze only the bulk speed hereafter. Figure 4 compares the break frequencies corresponding to the transition from the MHD to kinetic regime for the density (break point 2) and bulk speed spectra; the figure format is identical to Figure 3. Although both break points are almost identical when their frequencies are low (about 0.1–0.2 Hz), the speed break point is lower in a systematic way in the high-frequency range. For example, the density break point of 1 Hz roughly corresponds to the 0.3 Hz break point in the speed spectrum. Šafránková et al. (2015) have shown a linear dependence of the density break point on the gyrostructure frequency defined as $f_g = V_{\rm sw}/2\,\pi\,R_T$ where $V_{\rm sw}$ is the solar wind bulk speed and R_T is the proton thermal gyroradius, $R_T = V_{\rm th}/\omega_c$. This frequency has a good physical meaning because the spacecraft in the solar wind would observe such a frequency if the structures of size R_T are convected past.

A linear dependence of the density break point on this frequency suggests that the character of turbulence changes when the fluctuations become comparable to the proton gyroradius. Since the density break-point frequency changes by an order of magnitude but the solar wind speed only cahnges by a factor of two, the spatial dimensions of turbulent eddies are more important. In other words, the break-point frequency defines the smallest structures that could be supported by MHD processes under given conditions. This

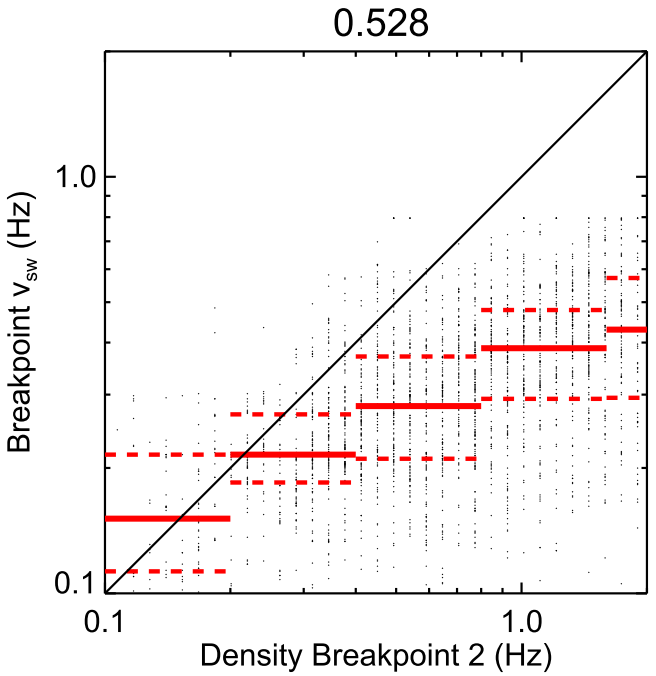

Figure 4. Comparison between the velocity break point and density break point 2. The red segments and diagonal line have the same meaning as in Figure 3.

simplified view can be applied on the velocity spectra but the density spectra exhibit two breaks and a plateau between them (Figure 1(c)). According to Chandran et al. (2009), the plateau in the density spectrum is caused by a dominance of kinetic Alfvén over MHD turbulence and, consequently, break point 2 is a characteristic of kinetic fluctuations rather than an indication of dissipation. Since the velocity break frequency is between the two breaks of the density spectrum, we can conclude that the breakdown of the MHD cascade happens in all fields in roughly the same place.

Chen et al. (2014a) argued that the break occurs at the gyrostructure frequency in high-β plasma but at the ion inertial length in the low-β environment. This conclusion was based on an analysis of magnetic field variations. To test whether or not

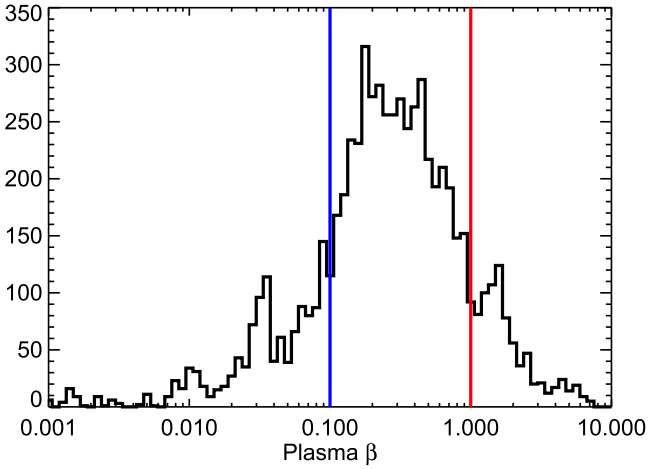

Figure 5. Distributions of β in our data set. The vertical lines mark the limits of the β analysis.

it can be used for speed fluctuations, we divided our set into three groups according to the ion β calculated from mean values of the magnetic field, proton temperature, and density on 20 minute intervals. The distribution of the averaged β representing our set is shown in Figure 5. As the histogram shows, the set does not contain intervals with extreme values of β, and thus we have chosen values of 0.1 and 1 as limits.

The scaling of the speed break point with the gyrostructure frequency is shown in Figure 6(a) for low (blue) and high (red) groups of β. Since the gyrostructure frequency is mainly determined by the magnitude of the magnetic field and the same holds for β, the two groups of β are well separated in the figure. The colored points show break points of individual spectra, and the heavy horizontal broken lines are medians in bins of the gyrostructure frequency. The intermediate values are denoted in black. The correlation coefficients above the panel are given for the full data set (black) and for particular subsets. One can see a relatively good scaling of the high-β events with the gyrostructure frequency and a little worse but still a good scaling of the low-β events.

An analogous analysis of a dependence of the break point on the inertial length frequency is shown in Figure 6(b). The inertial length frequency, f_L, is defined as the ratio $f_L = V_{sw}/\ 2\pi\ L$ where L is the inertial length. Surprisingly, the largest correlation coefficient between f_b and f_L was found for a group of high-β events. A slope of the dependence is close to unity. On the other hand, for the low-β events (blue), there is no correlation of the speed break point and inertial length frequency.

Chen et al. (2014a) suggested that the break point would be determined by the larger of two characteristic lengths; thus Figure 6(c) compares results of our analysis with this suggestion. Since inertial length frequency is typically smaller than gyrostructure frequency for small β, the blue points and lines (low-β events) are nearly the same as the symbols in Figure 6(b). The correlation coefficients are low (0.14), and thus we can conclude that the spectral break does not depend on the inertial length frequency for our low-β events. The gyrostructure frequency is usually lower for high-β events; thus a difference between red symbols in Figures 6(a) and (c) is negligible and the correlation coefficients are higher (0.43) in both panels.

Figure 6 apparently contradicts the suggestion of Chen et al. (2014a), but this suggestion was based on a discussion of events with $\beta > 10$ and/or $\beta < 0.03$. However, the number of such events in our set is too small and thus we are showing the ratios of the break-point frequency and characteristic frequencies (f_g and f_L) in Figure 7 as a function of β. The meaning of points and lines is the same as in previous figures. One can see that the ratio f_b/f_L tends toward unity with a decreasing β (Figure 7(a)), whereas the f_b/f_g ratio is about unity for several events with largest β (Figure 7(b)). The dependences of these ratios on β are very clear, the correlation coefficients given at the top of the panels are high (0.7 and 0.3 for f_b/f_g and f_b/f_L, respectively). However, both dependences are weak because, whereas a range of β is as broad as four orders of magnitude, the f_b/f_L ratio changes by a factor of about seven, and the f_b/f_g ratio by a factor of 20. Nevertheless, the dependences of normalized break frequencies on β in Figures 7(a) and (b) are opposite and thus a combination of these normalizations would be independent on β. Leamon et al. (1998) analyzed conditions for a cyclotron wave damping and suggested that $k_d = \omega\ /v_A + v_{th}$ is the minimum wavenumber at which the resonant dissipation would be important. This wavenumber corresponds to the frequency observed in the spacecraft frame, $f_d = V_{SW}/2\pi\ (L + R_g)$. Figure 7(c) shows the break frequency, f_b normalized to f_d as a function of ion β, and indeed, the plot does not exhibit any clear dependence; the correlation coefficient is very low.

Figure 7 suggests that a scaling of the bulk speed variations obeys similar rules as the scaling of magnetic field turbulence analyzed in Chen et al. (2014a). It is true for the extreme values of β analyzed there and probably for intermediate values as well. We cannot directly check this hypothesis due to the lack of magnetic field measurements on board *Spektr-R*.

Šafránková et al. (2015) has shown a very good correlation of the break frequency between MHD and kinetic scales with the gyrostructure frequency for solar wind density variations, but the dependence on β was not analyzed. Our set covers generally the same time intervals, and thus we present this analysis in Figure 8. The format of the figure is the same as that in Figure 7. A comparison of corresponding panels in both Figures 7 and 8 reveals the following.

1. The velocity break frequency is always lower than both the inertial length frequency and the gyrostructure frequency.
2. The density break frequency is always lower than the gyrostructure frequency, whereas it is above the inertial length frequency in low-β plasma and vice versa.
3. The density break frequency is larger than the speed break frequency; the difference decreases with β.
4. The density and speed break frequencies are both about equal to the gyrostructure frequency, f_g for very high (> 10) β. Whereas the application of the Leamon et al. (1998) scaling factor removes a dependence of the normalized break frequency on β for speed fluctuations, we did not succeed in finding a proper scaling for density fluctuations; f_g and f_d are roughly equivalent but a normalization with respect to f_g leads to a weaker dependence on β.

5. DISCUSSION AND CONCLUSION

This paper analyzes the shape and scaling of the power spectral densities of variations of the proton bulk and thermal

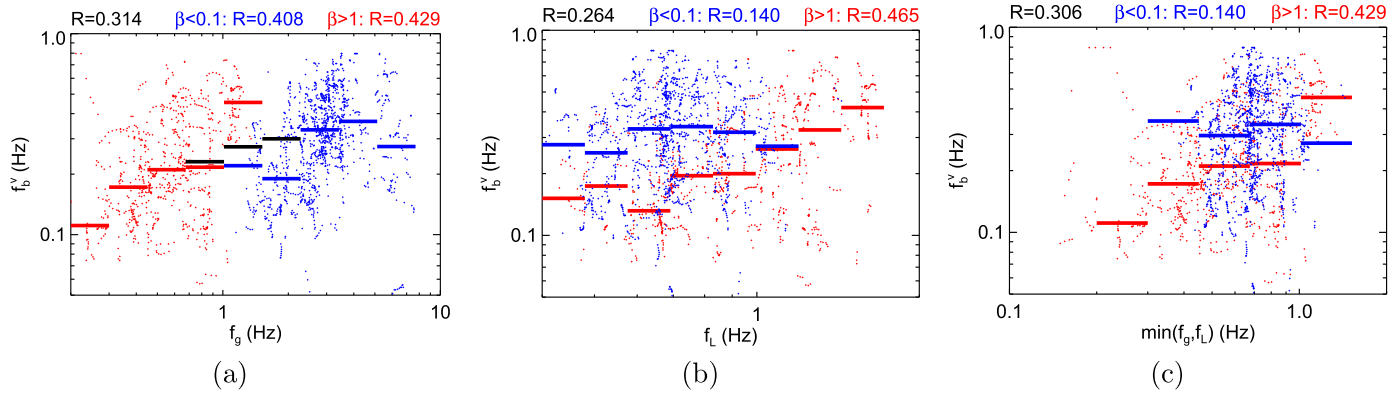

Figure 6. Scaling of velocity fluctuations as a function of ion β. The dependence of the velocity spectral break, f_b^V (a) on the gyro-structure frequency, f_g; on (b) inertial length frequency, f_L; and (c) on a minimal value of f_g and f_L frequencies. The blue and red points and lines mark two β ranges. The black line in panel (a) shows intermediate events. Above the panels, the correlation coefficients for all β (black), for low-β (blue), and for high-β (red) events are shown.

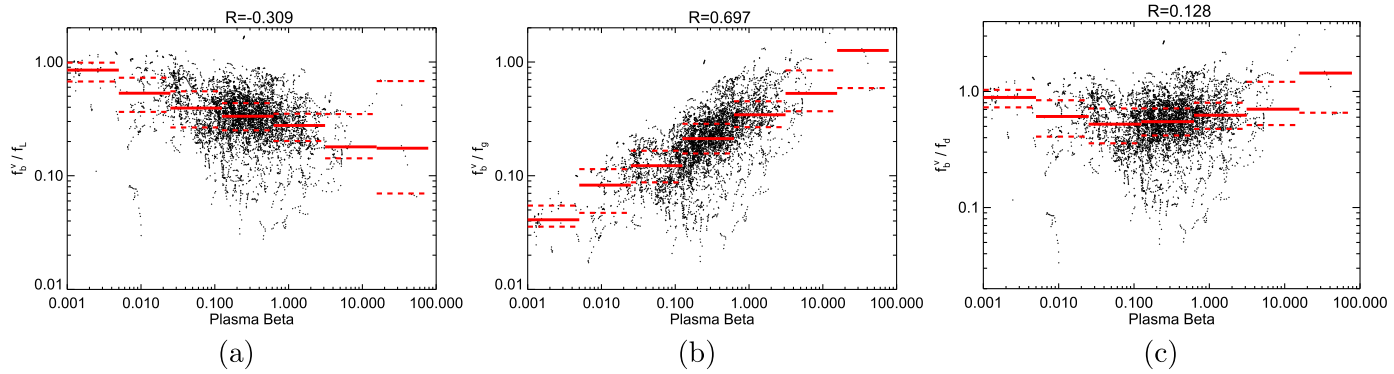

Figure 7. Scaling of normalized break points of velocity fluctuations according to ion β. The normalization is with respect to (a) the inertial length frequency, f_b^V/f_L; (b) the gyrostructure frequency, f_b^V/f_g; and (c) the f_d parameter (see the text for its explanation), f_b^V/f_d.

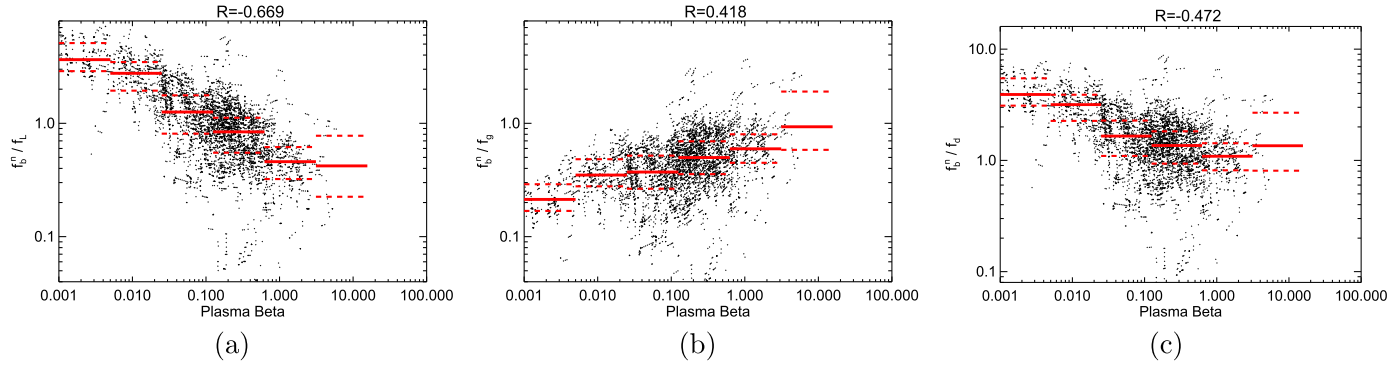

Figure 8. Scaling of normalized break points of density fluctuations according to ion β. The normalization is with respect to (a) the inertial length frequency, f_b^N/f_L; (b) the gyrostructure frequency, f_b^N/f_g; and (c) the f_d parameter, f_b^N/f_d.

speeds in the solar wind. Parameters of the frequency spectra of these quantities are compared with the analogous parameters of proton density spectra studied in Šafránková et al. (2015). The frequency ranges used in the present study (0.001–2 Hz for both bulk and thermal speeds and 0.001–8 Hz for density fluctuations) cover a transition from the MHD-governed scale to shorter scales where the kinetic processes become increasingly important. The results are relevant for the slow solar wind because the instrumental limitations of the BMSW instrument on board the *Spektr-R* spacecraft did not allow a reliable determination of speeds exceeding 570 km s^{-1}.

Similar to many previous studies, we have found that the PSD of speeds can be well approximated with two power-law segments divided by a clear break (Figures 1(a) and (b)). On the other hand, an analysis of the density variations (Figure 1(c)) revealed three power-law segments of the density spectrum, consistent with the study of Šafránková et al. (2015) and many other authors. It should be noted that the flattening of the speed spectra in the range of investigated frequencies was found neither for any individual spectrum nor for median spectra (Figure 2).

Figures 1 and 2 show that the spectra of bulk and thermal speeds are very similar. The slope of the bulk speed spectrum in the MHD range is close to the already suggested value of 3/2. Slightly different values obtained in our analysis (−1.47 in Figure 1 or 1.43 of the median spectrum in Figure 2) can be

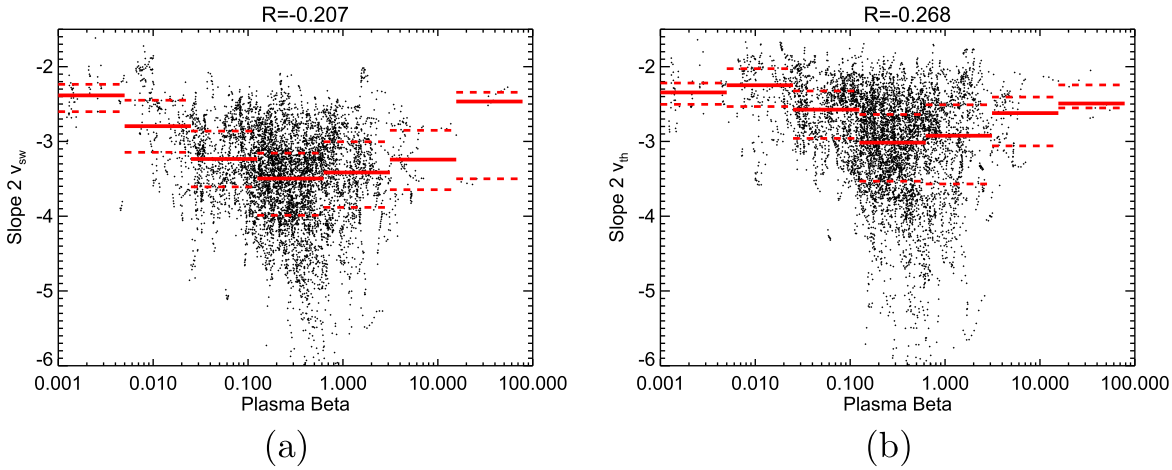

Figure 9. Dependence of slope 2 on (a) bulk and (b) thermal PSD spectra as a function of ion β.

probably attributed to a limited set of data and thus the already published discussions on the formation of this slope (Podesta & Borovsky 2010; Boldyrev et al. 2011b; Chen et al. 2011) can be applied.

A comparison of the spectral indices and break frequencies of bulk and thermal speed PSDs in Figure 3 demonstrates that there are no notable differences up to the end of the MHD range, but the spectrum of the thermal speed is more gradual at the kinetic range. The spectral indices at this range vary from -5 to -2 and differ by $\approx$0.5 with an exception of very flat spectra (Slope 2 of $V_{SW} > -2.5$ in Figure 3(c)). We searched for conditions typical for such slow dissipation and found that the flat spectra are observed when either the magnetic field or plasma density is high. This fact demonstrates the dependence of the spectral slopes of the bulk and thermal speeds on ion β, which is shown in Figure 9. Since it is generally believed that ion β is an important factor influencing the compressibility of the system and thus the nature of the investigated fluctuations (Servidio et al. 2015), the non-monotonic profiles of dependences in Figure 4 are surprising. There are two possible interpretations of the spectral steepening: (1) the slope increases due to a predominance of the forcing from large scales over dissipation (Šafránková et al. 2015), or (2) the slope becomes gradual if the dissipation weakens (e.g., Smith et al. 2006). Although these two interpretations are basically identical, the first of them underlines an increase of forcing, whereas the second accents the lack of dissipation. Since both the forcing and dissipation rates depend on ion β, their competition could lead to the non-monotonic change of the spectral slope with β. These effects are more pronounced for the bulk speed fluctuations; thus the spectral indices corresponding to the kinetic range of bulk and thermal speed fluctuations are about equal for extreme ion β values.

We have checked whether or not the already suggested scaling factors for a transition from the MHD to kinetic regime can be applied to the speed fluctuations and found that neither thermal proton gyroradius nor inertial length can be used for the whole range of β. Chen et al. (2014a) argued that this transition is controlled by the inertial length for very low β, whereas it occurs at the proton gyroradius in high-β plasma. This conclusion was supported with an analysis of magnetic field spectra and we have shown that it can be applied to the speed spectra as well. On the other hand, Figure 7(c) shows that the scaling suggested by Leamon et al. (1998) for cyclotron resonant wave damping can also be applied to the speed variations regardless of β. However, it is an open question whether or not cyclotron damping can act on low-frequency turbulence in the solar wind (Chen et al. 2014a).

The authors thank the *Wind* team for the magnetic field data. The BMSW data are available via http://aurora.troja.mff.cuni.cz/spektr-r/project/. This work was supported in part by the project LH15136 financed by the Ministry of Education of the Czech Republic, and in part by the Czech Science Foundation under Contract 16-04956S. C.H.K.C. was supported by an Imperial College Junior Research Fellowship.

Facility: Spektr-R.

REFERENCES

Alexandrova, O., Carbone, V., Veltri, P., & Sorriso-Valvo, L. 2008, ApJ, 74, 1153
Alexandrova, O., Saur, J., Lacombe, C., et al. 2009, PhRvL, 103, 165003
Belcher, J. W., & Davis, L. 1971, JGR, 76, 3534
Biskamp, D. 1993, Nonlinear Magnetohydrodynamics (Cambridge: Cambridge Univ. Press)
Boldyrev, S., & Perez, J. C. 2009, PhRvL, 103, 225001
Boldyrev, S., & Perez, J. C. 2012, ApJL, 758, L44
Boldyrev, S., Perez, J. C., Borovsky, J. E., & Podesta, J. J. 2011a, ApJ, 741, L19
Boldyrev, S., Perez, J. C., & Wang, Y. 2011b, in ASP Conf. Ser. 459, Numerical Modeling of Space Plasma Flows: ASTRONUM-2011 (San Francisco, CA: ASP), 3
Borovsky, J. E. 2012, JGR, 117, A05104
Bruno, R., & Carbone, V. 2013, LRSP, 10, 2
Chandran, B. D. G., Quataert, E., Howes, G., Xia, Q., & Pongkitiwanichakul, P. 2009, ApJ, 707, 1668
Chen, C. H. K., Bale, S. D., Salem, C., & Mozer, F. S. 2011, ApJL, 737, L41
Chen, C. H. K., Bale, S. D., Salem, C. S., & Maruca, B. A. 2013a, ApJ, 770, 125
Chen, C. H. K., Howes, G. G., Bonnell, J. W., et al. 2013b, in AIP Conf. Proc. 1539, SOLAR WIND 13: Proceedings of the Thirteenth International Solar Wind Conference (Melville, NY: AIP), 143
Chen, C. H. K., Leung, L., Boldyrev, S., Maruca, B. A., & Bale, S. D. 2014a, GeoRL, 41, 8081
Chen, C. H. K., Salem, C. S., Bonnell, J. W., Mozer, F. S., & Bale, S. D. 2012, PhRvL, 109, 035001
Chen, C. H. K., Sorriso-Valvo, L., Šafránková, J., & Němeček, Z. 2014b, ApJL, 789, L8
Goldreich, P., & Sridhar, S. 1995, ApJ, 438, 763
Grappin, R., Pouquet, A., & Leorat, J. 1983, A&A, 126, 51
Grappin, R., Velli, M., & Mangeney, A. 1991, AnGp, 9, 416

Howes, G. G. 2015, RSPTA, 373, 20140145
Kiyani, K. H., Chapman, S. C., Sahraoui, F., et al. 2013, ApJ, 763, 10
Leamon, R. J., Smith, C. W., Ness, N. F., Matthaeus, W. H., & Wong, H. K. 1998, JGR, 103, 4775
Mangeney, A., Salem, C., Veltri, P. L., & Cecconi, B. 2001, in Proc. ESA SP-492, Sheffield Space Plasma Meeting: Multipoint Measurements Versus Theory, ed. B. Warmbein (Noordwijk: ESA), 53
Matthaeus, W. H., & Goldstein, M. L. 1982, JGR, 87, 6011
Muller, W.-C., & Grappin, R. 2005, PhRvL, 95, 114502
Podesta, J. J., & Borovsky, J. E. 2010, PhPl, 17, 112905
Podesta, J. J., Roberts, D. A., & Goldstein, M. L. 2006, JGR, 111, A10109
Podesta, J. J., Roberts, D. A., & Goldstein, M. L. 2007, ApJ, 664, 543
Riazantseva, M. O., Budaev, V. P., Zelenyi, L. M., et al. 2015, RSPTA, 373, 20140146
Roberts, D. A. 2010, JGR, 115, A12101
Sahraoui, F., Goldstein, M. L., Robert, P., & Khotyaintsev, Y. V. 2009, PhRvL, 102, 231102
Salem, C., Mangeney, A., Bale, S. D., Veltri, P., & Bruno, R. 2007, in AIP Conf. Proc. 932, Turbulence and Nonlinear Processes in Astrophysical Plasmas, ed. D. Shaikh, & G. P. Zank (Melville, NY: AIP), 75
Salem, C. S., Howes, G. G., Sundkvist, D., et al. 2012, ApJL, 745, L9
Salem, C. S., Mangeney, A., Bale, S. D., & Veltri, P. 2009, ApJ, 702, 537
Servidio, S., Valentini, F., Perrone, D., et al. 2015, JPlPh, 81, 325810107
Smith, C. W., Hamilton, K., Vasquez, B. J., & Leamon, R. J. 2006, ApJL, 645, L85
Šafránková, J., Němeček, Z., Němec, F., et al. 2015, ApJ, 803, 107
Šafránková, J., Němeček, Z., Přech, L., & Zastenker, G. N. 2013a, PhRvL, 110, 025004
Šafránková, J., Němeček, Z., Přech, L., et al. 2013b, SSRv, 175, 165
Wang, Y., Boldyrev, S., & Perez, J. C. 2011, ApJL, 740, L36